The key genes involved in herpes simplex virus-1 corneal infection-induced acute hepatitis

Kai Hu [Corresp., Equal first author, 1], **Jinlong Li** [Equal first author, 2], **Xianwen Yuan** [3]

[1] Department of Ophthalmology, Nanjing Drum Tower Hospital, the Affiliated Hospital of Nanjing University Medical School, Nanjing University, Nanjing, China

[2] Department of Laboratory Medicine, The Second Hospital of Nanjing, Nanjing University of Chinese Medicine, Nanjing, China

[3] Department of Hepatobiliary Surgery, Nanjing Drum Tower Hospital, the Affiliated Hospital of Nanjing University Medical School, Nanjing University, Nanjing, China

Corresponding Author: Kai Hu
Email address: dahu0210@163.com

Background: Viral keratitis is mainly induced by herpes simplex virus (HSV). HSV-1 infection-induced acute hepatitis associates with immunodeficiency. Related biomarkers have not been systemically identified till now. This study was designed to explore the molecular mechanisms and potential biomarkers of HSV-1 infection-induced acute hepatitis. ***Methods:*** Microarray dataset GSE35943, including the liver tissues infected by HSV-1 (1, 3, 5, and 7 days post infection) and the corresponding control tissues, was extracted from Gene Expression Omnibus database. The differentially expressed genes (DEGs) were identified using and were clustered using time series expression analysis. DEG-associated KEGG pathways were called using online DAVID tool. Using Cytoscape software, protein-protein interaction (PPI) network was built and significant network modules were identified. ***Results:*** A total of 2909 DEGs grouping into 3 clusters with similar gene expression profiles were obtained. The DEGs were involved in immune-associated functional terms and pathways like natural killer cell mediated cytotoxicity and antigen processing and presentation. DEGs including PIK3R1, PIK3CD, PLCG2, PTPN6, LCK, RAC2, and PLK1 had higher degrees in the PPI network and 8 significant modules. ***Conclusion:*** *PIK3R1*, *PIK3CD*, *PLCG2*, *PTPN6*, *LCK*, *RAC2* and *PLK1* were identified to be associated with HSV-1 corneal infection-induced hepatitis, and might be potential clinical biomarkers for the diagnosis of HSV-1-induced hepatitis.

The key genes involved in herpes simplex virus-1 corneal infection-induced acute hepatitis

Running title: Genes in HSV-1 hepatitis

Kai Hu[1,2,*,§], Jinlong Li[3,§], Xianwen Yuan[4]

1 Department of Ophthalmology, Nanjing Drum Tower Hospital, Medical Collage of Nanjing University, Nanjing, 210008, P. R. China
2 Nanjing Ningyi Eye Center, Nanjing, P. R. China
3 Department of Laboratory Medicine, the Second Hospital of Nanjing, Nanjing University of Chinese Medicine, Nanjing 210003, P. R. China
4 Department of Hepatobiliary Surgery, Nanjing Drum Tower Hospital, Medical Collage of Nanjing University, Nanjing, 210008, P. R. China

§ equal contribution.
Corresponding author: Dr. Kai Hu.
E-mail: dahu0210@163.com;
Address: Department of Ophthalmology, Nanjing Drum Tower Hospital, Medical Collage of Nanjing University, No. 321 Zhongshan Road, Gulou District, Nanjing, 210008 Jiangsu, China.

Highlights:

1. There an overall 2909 dysregulated genes in different groups.

2. Cluster 4, 6, and 8 showed similar expression trends.

3. PIK3R1, PIK3CD, PLCG2, PTPN6, LCK, RAC2, and PLK1 were key network nodes.

Abstract

Background: Viral keratitis is mainly induced by herpes simplex virus (HSV). HSV-1 infection-induced acute hepatitis associates with immunodeficiency. Related biomarkers have not been systemically identified till now. This study was designed to explore the molecular mechanisms and potential biomarkers of HSV-1 infection-induced acute hepatitis.

Methods: Microarray dataset GSE35943, including the liver tissues infected by HSV-1 (1, 3, 5, and 7 days post infection) and the corresponding control tissues, was extracted from Gene Expression Omnibus database. The differentially expressed genes (DEGs) were identified using and were clustered using time series expression analysis. DEG-associated KEGG pathways were called using online DAVID tool. Using Cytoscape software, protein-protein interaction (PPI) network was built and significant network modules were identified.

Results: A total of 2909 DEGs grouping into 3 clusters with similar gene expression profiles were obtained. The DEGs were involved in immune-associated functional terms and pathways like natural killer cell mediated cytotoxicity and antigen processing and presentation. DEGs including PIK3R1, PIK3CD, PLCG2, PTPN6, LCK, RAC2, and PLK1 had higher degrees in the PPI network and 8 significant modules.

Conclusion: *PIK3R1*, *PIK3CD*, *PLCG2*, *PTPN6*, *LCK*, *RAC2* and *PLK1* were identified to be associated with HSV-1 corneal infection-induced hepatitis, and might be potential clinical biomarkers for the diagnosis of HSV-1-induced hepatitis.

Introduction

Keratitis is a condition of inflamed cornea (Furlanetto et al. 2010). Keratitis is usually characterized by pain, photophobia, visual impairment, gritty sensation and red eye (Zapp et al. 2018). According to the sources of infection, keratitis can be divided into viral, bacterial, fungal , amoebic and parasitic keratitis (Clarke et al. 2012; Ritterband 2014; Tang et al. 2009). Infectious keratitis often deteriorates rapidly and needs urgent antiviral, antibacterial or antifungal therapy (Morén et al. 2010). Without proper and timely treatment, infectious keratitis may lead to impaired eyesight, corneal perforation, or even loss of vision (Hassairi et al.

2016).

Among viral sources of keratitis, ophthalmic herpes simplex virus (HSV) is an important leading cause of ocular manifestations, including corneal opacification and stromal keratitis and indication of penetrating keratoplasty (Knickelbein et al. 2009; M et al. 2016). HSV is the earliest isolated herpes virus in the 1930s, and humans are the only natural reservoir of this virus (Wald & Ashleymorrow 2002). HSV is a double-stranded DNA virus, which can be divided into HSV-1 and HSV-2 (Kolb et al. 2013). Brain is one of the HSV-1-affected organ in human. HSV-1 causes encephalitis in immune-suppressed hosts and human herpes simplex encephalitis (HSE) is the most frequent form of viral sporadic encephalitis (Pasieka et al. 2011). With the increase in the incidence of immunodeficiency diseases and the increase in the resistance of HSV to antiviral drugs, the treatment for HSV-1—induced acute diseases becomes more difficult and the disease begins to receive attention.

Previous studies commonly focused on HSE, and rarely on liver HSV-1 infection (Katzenell et al. 2014; Kurt-Jones et al. 2004; Pasieka et al. 2011; Thaís et al. 2014). The liver is another major organ affected by HSV-1 (Pasieka et al. 2011). The first HSV hepatitis was reported in 1969 (FLEWETT et al. 1969). Since then, HSV hepatitis has been gradually diagnosed. Hepatitis refers to the inflammation derived from the liver, which is divided into acute (continuing for under six months) and chronic hepatitis (lasting for over six months) (Maasoumy & Wedemeyer 2012). Hepatitis is usually induced by virus infection (including hepatitis B virus), toxins, some medications, autoimmune diseases and other factors (Ayako et al. 2017; Pianko et al. 2010). It has been reported that the HSV infection rarely induces hepatitis, and often occurs after liver transplantation and leads to acute liver failure (Liebau et al. 1996; Norvell et al. 2010). Impaired immunity resulting from immunosuppression after liver transplantation, inhalational anesthetics, pregnancy and malignancy may be

predisposing factor of HSV hepatitis (Kaufman et al. 1997). It has been reported *in vivo* in animal experiments that HSV-1 infection in *Stat1*-knockout mice from eyes reduced the survival time significantly with significant liver lesions (Katzenell et al. 2014; Pasieka et al. 2011).

In immune-suppressed hosts, HSV-1 causes acute hepatitis (Pasieka et al. 2011). The main clinical presentations of HSV-induced hepatitis were fever, encephalopathy, coagulopathy and rash (Norvell et al. 2010), which commonly lead to the misdiagnosis of HSV hepatitis. The high mortality of HSV hepatitis could be reduced if being diagnosed expeditiously and treated properly. Therefore, diagnostic biomarkers on presentation the course of HSV hepatitis would be of great value for clinicians.

Through analyzing the dynamic change of gene expression levels in liver tissues from mice infected corneally by HSV-1, the key genes acting in HSV-1 corneal infection-induced hepatitis were screened. This study might contribute to revealing the mechanisms of HSV-1 corneal infection-induced hepatitis in immunodeficient mice and providing the basis for the clinical diagnosis of HSV-1-induced hepatitis.

Materials and Methods

Microarray data and data pretreatment

The gene expression profile under GSE35943, which was sequenced on the platform of GPL7202 Agilent-014868 Whole Mouse Genome Microarray 4x44K G4122F (Probe Name version), was obtained from Gene Expression Omnibus (GEO, http://www.ncbi.nlm.nih.gov/geo/) database. In the dataset, the liver tissues from immunocompetent mice (Stat1$^{-/-}$ strain) infected corneally by HSV-1 (KOS and an attenuated recombinant virus lacking the vhs function, Δvhs) for 1, 3, 5 and 7 days (each time point contained 4 samples) and the liver tissues from control mice (129S6 strain) with normal growth on the corresponding days (each time point included 2 samples) were selected as the analysis objects. The microarray dataset GSE35943 was

extracted from public database, therefore, ethical review and patient consent were not needed.

Using the R package limma (Ritchie et al. 2015) (version 3.34.0, https://bioconductor.org/packages/release/bioc/html/limma.html), the original data in TXT format was conducted with log2 conversion and data normalization.

Differential expression analysis

According to the time points of sample collection, the samples were divided into four time point groups (D1, D3, D5 and D7). Based on the R package limma (Ritchie et al. 2015), the differentially expressed genes (DEGs) between HSV-1 infected samples and control samples were analyzed for each time point group. The false discovery rate (FDR) < 0.05 and $|\log_2 \text{fold change (FC)}| > 0.263$ were used as the thresholds for screening DEGs. Combined with Venn diagram (Shamansky & Graham 2010), the DEGs of the four time point groups were compared and their union were obtained for further analyses.

Time series expression analysis and enrichment analysis

Short Time-series Expression Miner (STEM, version 1.3.11, http://www.cs.cmu.edu/~jernst/stem/) is the first software program specifically designed for the analysis of short time series microarray data, which clusters, compares and visualizes these data (Ernst & Bar-Joseph 2006). Using STEM software (Ernst & Bar-Joseph 2006), the union of the DEGs were conducted with time series expression analysis under the significant criteria of FDR < 0.05 and similarity > 0.6.

Then, the clusters with significantly similar expression trends were conducted with Gene Ontology (GO) (Balakrishnan et al. 2013) and Kyoto Encyclopedia of Genes and Genomes (KEGG) (H et al. 2000) enrichment analyses using DAVID tool (Da Wei et al. 2009) (version 6.8, https://david.ncifcrf.gov/). The FDR < 0.05 was selected as the screening threshold.

Protein-protein interaction (PPI) network construction and analysis

Combined with STRING database (Damian et al. 2011) (version 10.0, http://string-db.org), the PPIs among the protein products of the DEGs were searched. Subsequently, the PPI network was visualized by Cytoscape software (Lopes et al. 2010) (version 3.6.1, http://www.cytoscape.org/). Using the Molecular Complex Detection (Mcode; parameters: Degree cutoff = 2, Node score cutoff = 0.2, K-core = 2) plug-in (Hwang et al. 2006) in Cytoscape software, network modules were divided and identified.

The vast majority of biological networks are subject to scale-free network property, that is to say a few nodes (hub nodes) in the network have a large number of connections, and most nodes only have a small number of connections (Jeong et al. 2001). The topology of the constructed PPI network was analyzed, and four important network topology parameters (including degree; betweenness centrality, BC; closeness centrality, CC; and path length) were calculated.

Results

Data pretreatment and differential expression analysis

The original data was pretreated, and the box plots before and after normalization was presented in Figure 1. There were 430 (83 up-regulated genes and 347 down-regulated genes), 1198 (414 up-regulated genes and 784 down-regulated genes), 989 (378 up-regulated genes and 611 down-regulated genes), and 628 (214 up-regulated genes and 414 down-regulated genes) DEGs between HSV-1 infected samples and control samples in D1, D3, D5 and D7 time point groups, respectively (Figure 2A). A total of 2909 non-overlapping DEGs were acquired (Figure 2B). The DEGs in each time point are listed in Table S1.

Time series expression analysis and enrichment analysis

, Time series expression analysis was performed based on the expression levels of the 2909 DEGs. Three

clusters with significantly similar expression trends ($p<0.05$) were obtained, including cluster 4 (involving 345 DEGs), cluster 6 (involving 295 DEGs), cluster 8 (involving 759 DEGs) (Figure 3).

Enrichment analysis indicated that these DEGs were implicated in 8 GO terms (including immune response, and antigen processing and presentation of exogenous peptide antigen) and 7 KEGG pathways (including natural killer cell mediated cytotoxicity, and antigen processing and presentation; Table 1). Detail information of pathways and genes are shown in Table S2.

PPI network analysis

In the PPI network constructed for the DEGs in the three clusters, there were 502 nodes (gene productions) and 1505 edges (interactions; Figure 4). Enrichment analysis was conducted for the 502 nodes. A total of 15 GO terms (including immune response, defense response, and cell activation) and 13 KEGG pathways (including natural killer cell mediated cytotoxicity, antigen processing and presentation, and cytokine-cytokine receptor interaction) were enriched (Table 2). The topology parameters of the top 10 network nodes (including phosphatidylinositol 3-kinase regulatory subunit 1, PIK3R1 (down, D1); phosphoinositide-3 kinase, catalytic subunit delta, PIK3CD (up, D3); phospholipase C gamma-2, PLCG2 (up, D3); protein tyrosine phosphatase nonreceptor type 6, PTPN6 (down, D3); lymphocyte-specific protein tyrosine kinase, LCK (up, D5); Ras-related C3 botulinum toxin substrate 2, RAC2 (up, D3); polo-like kinase 1, PLK1 (up, D3)) are listed in Table 3. Importantly, PIK3R1 had interactions with PIK3CD, PLCG2, PTPN6, LCK, and RAC2 in the PPI network. Detail with gene information is seen in Table S3.

Eight significant modules were obtained from the PPI network (Table 4, Figure 5). Moreover, the genes involved in module 1, 2, 3, 4, 5, 6, 7, and 8 were separately enriched in 17 (including sensory perception of smell), 11 (such as G-protein coupled receptor protein signaling pathway), 23 (including immune system

process), 8 (such as response to wounding), 11 (such as protein modification by small protein conjugation), 10 (such as mRNA metabolic process), 9 (such as protein transport), and 10 (such as cellular process) GO terms.

Discussion

In this study, 430, 1198, 989, and 628 DEGs were separately identified in D1, D3, D5 and D7 time point groups, overall 2909 non-overlapping DEGs. These DEGs were clustered into 3 clusters (cluster 4, 6, and 8) with similar expression profiles. Enrichment analysis showed DEGs were involved in immune-associated GO terms and KEGG pathways. Further analysis using the PPI network showed key nodes like PIK3R1, PIK3CD, PLCG2, PTPN6, LCK, RAC2, and PLK1 might be key candidates in HSV-1. These results showed that the HSV-1 infection in eyes in immunodeficient mice induced acute liver disease.

Among these DEGs, key candidates including *RAC2*, and *PLK1* showed interesting roles in HSV-1 infection-related hepatitis. These genes, like *PLCG2* and *RAC2* had been reported to be associated with immunity and inflammation directly or indirectly. Through mediating the tyrosine phosphorylation of *PLCG2*, epidermal growth factor (*EGF*) promotes the activity of *PLCG1* in corneal epithelial cells of rabbit (Islam & Akhtar 2000). The tyrosine kinase *PLCG2* acts in the early stage of innate immunity, and is implicated in cytokine production and Ca^{2+} flux in corneal epithelial cells infected by *Aspergillus fumigatus* (Di et al. 2016; Peng et al. 2018). In addition, *PLCG* and focal adhesion kinase (*FAK*) are implicated in mediating hepatic stellate cell (HSC) adhesion and motility (Carloni et al. 1997). *RAC1* correlates with inflammatory and fibrotic stress response in the liver of mice receiving doxorubicin (Bopp A 2013). Through conducting transforming growth factor β1 (*TGF-β1*) signaling to PI3Kγ/AKT/RAC1 pathway, 14 kDa phosphohistidine phosphatase (*PHP14*) mediates the migration of HSCs and functions in liver fibrosis (Choi et al. 2010; Xu et al. 2017). The cell division cycle protein 42 (Cdc42)/Rac pathway is influenced by the HSV-2-produced unique short region

177 3 (US3) protein kinase (PK) , which inhibits the activation of c-Jun N-terminal kinase (T et al. 2010). Up-
178 regulated *Rac2*, as well as down-regulated *paxillin*, *RhoA* and *CD18* in peripheral blood may play critical roles
179 in corneal graft rejection (M-C et al. 2009; Ortega et al. 2016). Moreover, The guanosine triphosphatase *RAC2*
180 acts in the mediation of reactive oxygen species (ROS) and is important for carbon tetrachloride (CCl4)-
181 associated acute liver injury (Zou et al. 2017). Both PLCG2 and RAC2 were upregulated in liver tissues at day
182 3 post corneal HSV-1 infection. These results showed that *PLCG2* and *RAC2* were correlated with and might
183 have crucial roles in HSV-1 corneal infection-induced liver lesion.
184
185 Other DEGs, including *PIK3R1*, *PIK3CD*, *PLCG2*, *PTPN6* and *LCK* showed interest roles in HSV-1
186 corneal infection-induced hepatitis. Based on *LCK* activation, hepatitis C virus (HCV) envelope protein E2
187 binds to *CD81* and exerts costimulatory roles on T cells and results in increased T cell antigen receptor (TCR)
188 signaling (Soldaini et al. 2010). *C1q* (a ligand of complement component C1q (*gC1qR*)) inhibits proliferation
189 of T cells through binding to them, and damaged T-cell function and Lck/Akt activation are induced by the
190 direct binding of HCV core to *gC1qR* (Zhi Qiang et al. 2004). The nonstructural protein 5A (NS5A)
191 phosphokinase *PLK1* indirectly mediates the RNA replication of HCV and plays differential roles in host cell
192 growth and HCV replication, indicating that *PLK1* can be a promising target for anti-HCV treatment (Yung-
193 Chia et al. 2010). As a proviral host factor, *PLK1* can be used for the therapies of hepatitis B virus (HBV)
194 infection and HBV-induced carcinogenesis (Diab et al. 2017). Via activating the PLK3 pathway, hyperosmotic
195 stress (increased extracellular solute concentration) enhances the phosphorylation of activating transcription
196 factor-2 (*ATF-2*) in human corneal epithelial cells (Wang et al. 2011b). In addition, Plk3 gene is upregulated in
197 liver biopsies of HBV-infected patients in inactive carrier status phase relative to active chronic hepatitis phase

198 (Liu et al. 2018). *PLK3* and *c-Jun* can be activated by hyperosmotic and oxidative stresses (Wang et al. 2011a;
199 Zhong et al. 2017), and c-JUN promotes HBV-related hepatocellular carcinoma (HCC) tumorigenesis and
200 autophagy in mice (Trierweiler et al. 2013; Zhong et al. 2017). These results revealed the crucial roles of *LCK*,
201 *PLK1* and *PLK3* in HBV and HCV-induced liver diseases. The present study found LCK and PLK1 were
202 upregulated in livers tissues at day 5 and day 3, respectively, post HSV-1 corneal infection. The dysregulated
203 expression of both genes suggested that they might play important roles in HSV-1 corneal infection-induced
204 hepatitis.
205
206 Through suppressing *PIK3*, adenosine 3',5'-monophosphate (*cAMP*) regulates the expression of *p27* and
207 cyclin-dependent kinase 4 (*CDK4*) and represses corneal endothelial cell proliferation (Lee & Kay 2003).
208 Pseudopodia formation and membrane fusion are critical steps for HSV-1 entry into cells, and PIK3 signaling
209 may have influences on these steps by affecting RhoA activation (Kai et al. 2014; Tiwari & Shukla 2010).
210 *PIK3-γ* plays a critical role in the activation and recruitment of inflammatory cells, and the selective PIK3-γ
211 inhibitor AS605240 may be applied for the therapy of concanavalin A (ConA)-induced liver damage (Zhen-
212 Ling et al. 2009). Deficiency in small heterodimer partner (*SHP*, also named *PTPN6*) /Src homology region 2
213 domain-containing phosphatase 1 (*SHP1*) is related to human inflammatory diseases and is bad for controlling
214 bacterial infection (Zakia et al. 2013). Via targeting the *SHP*/*PTPN6* phosphatase, sorafenib significantly
215 represses the hepatitis B X (HBx)-enhanced androgen receptor activity and may be applied for the
216 chemoprevention of HBV-correlated HCC (Wang et al. 2015). Mutations in the PIK3R1 and PIK3CD gene
217 cause human immunodeficiency (Dornan et al. 2017; Marie-Céline et al. 2014). Marie-Céline et al showed
218 PIK3R1 mutations inhibited p110 activity, decreased naive T and memory B cell counts in blood, promoted T

cell blasts activation-induced cell death. Therefore, *PIK3*, *PIK3R1*, *PIK3CD*, and *PTPN6* were associated with the mechanisms of HSV-1 corneal infection-induced liver diseases. In the present study, PIK3R1 was downregulated in liver on day 1 post HSV-1 infection, which might correlate with the Stat1 knockout-induced immunodeficiency in mice. We found PIK3R1 interacted with PIK3CD (up on day 3), PLCG2 (up on day 3), PTPN6 (down on day 3), LCK (up on day 5), and RAC2 (up on day 3) in the PPI network were mostly dysregulated in livers on day 3 post HSV-1 infection, and all interacted with each other and PIK3R1 in PPI network and modules. These results indicated that *PIK3R1* and its interacting genes PIK3CD, PLCG2, PTPN6, LCK and RAC1 took crucial roles in HSV-1 infection-induced hepatitis or liver hepatitis.

Conclusions

In conclusion, 2909 DEGs in the HSV-1 corneal infection-induced hepatitis were obtained. Among them, *PIK3R1*, *PIK3CD*, *PLCG2*, *PTPN6*, *LCK*, *RAC2*, and *PLK1* might correlate with the pathogenesis and development of HSV-1 infection-induced hepatitis and human immunodeficiency. Experimental researches may support the roles of these key genes in HSV-1 infection-induced acute hepatitis. Clinics trials may testify whether these genes could be used as the clinical biomarkers for diagnosis of HSV-1-induced hepatitis or not.

Supplementary files

Table S1. The DEGs list.

Table S2. Enrichment analysis for the DEGs involved in the three clusters.

Table S3. The result of enrichment analysis for the nodes in the protein-protein interaction (PPI) network.

References

Ayako, Iida-Ueno, Masaru, Enomoto, Akihiro, Tamori, Norifumi, and Kawada. 2017. Hepatitis B virus infection and alcohol consumption. *World Journal of Gastroenterology* 23:2651-2659.

Balakrishnan R, Harris MA, Huntley R, Van AK, and Cherry JM. 2013. A guide to best practices for Gene Ontology (GO) manual annotation. *Database,2013,(2013-01-01)* 2013:2681-2694.

Bopp A WF, Henninger C , et al. 2013. Rac1 modulates acute and subacute genotoxin-induced hepatic stress responses, fibrosis and liver aging. . *Cell Death & Disease* 4:e558.

Carloni V, Romanelli RG, Pinzani M, Laffi G, and Gentilini P. 1997. Focal adhesion kinase and phospholipase C gamma involvement in adhesion and migration of human hepatic stellate cells. *Gastroenterology* 112:522.

Choi SS, Sicklick JK, Qi M, Liu Y, Jiawen H, Yi Q, Wei C, Yin-Xiong L, Goldschmidt-Clermont PJ, and Anna Mae D. 2010. Sustained activation of Rac1 in hepatic stellate cells promotes liver injury and fibrosis in mice. *Hepatology* 44:1267-1277.

Clarke B, Sinha A, Parmar DN, and Sykakis E. 2012. Advances in the diagnosis and treatment of acanthamoeba keratitis. *Journal of Ophthalmology* 2012:484892.

Da Wei H, Sherman BT, and Lempicki RA. 2009. Bioinformatics enrichment tools: paths toward the comprehensive functional analysis of large gene lists. *Nucleic Acids Research* 37:1.

Damian S, Andrea F, Michael K, Milan S, Alexander R, Pablo M, Tobias D, Manuel S, Jean M, and Peer B. 2011. The STRING database in 2011: functional interaction networks of proteins, globally integrated and scored. *Nucleic Acids Research* 39:561-568.

Di ZA, Tahvildari M, Florakis GJ, and Dana R. 2016. Ocular Manifestations of Inherited Phospholipase-Cγ2-Associated Antibody Deficiency and Immune Dysregulation. *Cornea* 35.

Diab AM, Foca A, Fusil F, Lahlali T, Jalaguier P, Amirache F, N'Guyen L, Isorce N, Cosset FL, and Zoulim F. 2017. Polo-like-kinase 1 is a proviral host-factor for hepatitis B virus replication. *Hepatology* 66.

Dornan GL, Siempelkamp BD, Jenkins ML, Vadas O, Lucas CL, and Burke JE. 2017. Conformational disruption of PI3KÎ´ regulation by immunodeficiency mutations in PIK3CD and PIK3R1. *Proc Natl Acad Sci U S A* 114:1982-1987.

Ernst J, and Bar-Joseph Z. 2006. STEM: a tool for the analysis of short time series gene expression data. *Bmc Bioinformatics* 7:1-11.

FLEWETT TH, PARKER RGF, and PHILIP WM. 1969. Acute hepatitis due to Herpes simplex virus in an adult. *Journal of Clinical Pathology* 22:60.

Furlanetto RL, Arcieri E, Ferreira MA, and Rocha FJ. 2010. Epidemiology and etiologic diagnosis of infectious keratitis in Uberlandia, Brazil. *European Journal of Ophthalmology* 20:498.

H O, S G, K S, W F, H B, and M K. 2000. KEGG: Kyoto Encyclopedia of Genes and Genomes. *Nucleic Acids Research* 27:29-34.

Hassairi A, Limaiem R, Mrad AB, Rayhan H, Turki R, and Matri LE. 2016. Infectious keratitis after penetrating keratoplasty: predisposing risk factors and prognosis. *Acta Ophthalmologica* 94.

Hwang W, Cho YR, Zhang A, and Ramanathan M. 2006. A novel functional module detection algorithm for protein-protein interaction networks. *Algorithms for Molecular Biology* 1:24-24.

Islam M, and Akhtar RA. 2000. Epidermal Growth Factor Stimulates Phospholipase Cγ1 in Cultured Rabbit Corneal Epithelial Cells. *Experimental Eye Research* 70:261-269.

Jeong H, ., Mason SP, Barabási AL, and Oltvai ZN. 2001. Lethality and centrality in protein networks. *Nature*

411:41-42.

Kai Z, Yangfei X, Xiao W, Qiaoli W, Meigong Z, Shaoxiang W, Xiaoyan W, Jianglin F, Kaio K, and Yifei W. 2014. Epidermal growth factor receptor-PI3K signaling controls cofilin activity to facilitate herpes simplex virus 1 entry into neuronal cells. *Mbio* 5:e00958.

Katzenell S, Chen Y, Parker ZM, and Leib DA. 2014. The differential interferon responses of two strains of Stat1-deficient mice do not alter susceptibility to HSV-1 and VSV in vivo. *Virology* 450-451:350-354.

Kaufman B, Gandhi SE, Rizzi R, and Illei P. 1997. Herpes simplex virus hepatitis: case report and review. *Clinical Infectious Diseases* 24:334-338.

Knickelbein JE, Hendricks RL, and Charukamnoetkanok P. 2009. Management of Herpes Simplex Virus Stromal Keratitis: An Evidence-based Review. *Survey of Ophthalmology* 54:226-234.

Kolb AW, Ané C, and Brandt CR. 2013. Using HSV-1 Genome Phylogenetics to Track Past Human Migrations. *Plos One* 8:e76267.

Kurt-Jones EA, Melvin C, Shenghua Z, Jennifer W, George R, Roderick B, Arnold MM, Knipe DM, and Finberg RW. 2004. Herpes simplex virus 1 interaction with Toll-like receptor 2 contributes to lethal encephalitis. *Proc Natl Acad Sci U S A* 101:1315-1320.

Lee HT, and Kay EP. 2003. Regulatory role of cAMP on expression of Cdk4 and p27(Kip1) by inhibiting phosphatidylinositol 3-kinase in corneal endothelial cells. *Investigative Ophthalmology & Visual Science* 44:3816-3825.

Liebau MP, Kuse ME, Winkler MM, Schlitt PMHJ, Oldhafer PMK, Pichlmayr MR, Verhagen MW, and Flik MJ. 1996. Management of herpes simplex virus type 1 pneumonia following liver transplantation. *Infection* 24:130-135.

Liu H, Li F, Zhang X, Yu J, Wang J, Jia J, Yu X, Shen Z, and Yuan Z. 2018. Differentially expressed intrahepatic genes contribute to control of hepatitis B virus replication in the inactive carrier phase. *Journal of Infectious Diseases* 217:DOI: 10.1093/infdis/jix1683.

Lopes CT, Farzana K, Donaldson SL, Quaid M, and Bader GD. 2010. Cytoscape Web: an interactive web-based network browser. *Bioinformatics* 26:2347-2348.

M-C H, Tullo AB, and Hillarby MC. 2009. Increased Rac2 mRNA expression in peripheral blood during human corneal graft rejection. *Eye* 23:461.

M T, C M, I A, MM M, P H, and D A. 2016. Herpes simplex virus keratitis: an update of the pathogenesis and current treatment with oral and topical antiviral agents. *Clinical and Experimental Ophthalmology* 44:824-837.

Maasoumy B, and Wedemeyer H. 2012. Natural history of acute and chronic hepatitis C. *Best Practice & Research Clinical Gastroenterology* 26:401-412.

Marie-Céline D, Lucie H, Pierre F, Felipe S, Christine B-F, Patrick N, Marina C, Capucine P, Anne D, and Alain F. 2014. A human immunodeficiency caused by mutations in the PIK3R1 gene. *Journal of Clinical Investigation* 124:3923.

Morén H, Malmsjö M, Mortensen J, and Ohrström A. 2010. Riboflavin and ultraviolet a collagen crosslinking of the cornea for the treatment of keratitis. *Cornea* 29:102.

Norvell JP, Blei AT, Jovanovic BD, and Levitsky J. 2010. Herpes simplex virus hepatitis: an analysis of the published literature and institutional cases. *Liver Transpl* 13:1428-1434.

Ortega MC, Santander-García D, Marcos-Ramiro B, Barroso S, Cox S, Jiménez-Alfaro I, and Millán J. 2016.

Activation of Rac1 and RhoA Preserve Corneal Endothelial Barrier Function. *Investigative Ophthalmology & Visual Science* 57:6210.

Pasieka TJ, Cilloniz C, Carter VS, Rosato P, Katze MG, and Leib DA. 2011. Functional Genomics Reveals an Essential and Specific Role for Stat1 in Protection of the Central Nervous System following Herpes Simplex Virus Corneal Infection. *Journal of Virology* 85:12972-12981.

Peng X, Zhao G, Lin J, Qu J, Zhang Y, and Li C. 2018. Phospholipase Cγ2 is critical for Ca 2+ flux and cytokine production in anti-fungal innate immunity of human corneal epithelial cells. *Bmc Ophthalmology* 18:170.

Pianko S, Patella S, Ostapowicz G, Desmond P, and Sievert W. 2010. Fas-mediated hepatocyte apoptosis is increased by hepatitis C virus infection and alcohol consumption, and may be associated with hepatic fibrosis: mechanisms of liver cell injury in chronic hepatitis C virus infection. *Journal of Viral Hepatitis* 8:406-413.

Ritchie ME, Belinda P, Di W, Yifang H, Law CW, Wei S, and Smyth GK. 2015. limma powers differential expression analyses for RNA-sequencing and microarray studies. *Nucleic Acids Research* 43:e47.

Ritterband DC. 2014. Herpes simplex keratitis: classification, pathogenesis and therapy. *Expert Review of Ophthalmology* volume 1:241-256.

Shamansky SL, and Graham KY. 2010. The Venn diagram: a metaphor for life. *Public Health Nursing* 16:1-2.

Soldaini E, Wack A, D'Oro U, Nuti S, Ulivieri C, Cosima, #x, Baldari T, and Abrignani S. 2010. T cell costimulation by the hepatitis C virus envelope protein E2 binding to CD81 is mediated by Lck. *European Journal of Immunology* 33:455-464.

T M, F G, T D, H T, and Y N. 2010. Expression of herpes simplex virus type 2 US3 affects the Cdc42/Rac pathway and attenuates c-Jun N-terminal kinase activation. *Genes to Cells* 5:1017-1027.

Tang A, Marquart ME, Fratkin JD, Mccormick CC, Caballero AR, Gatlin HP, and O'Callaghan RJ. 2009. Properties of PASP: a Pseudomonas protease capable of mediating corneal erosions. *Investigative Ophthalmology & Visual Science* 50:3794.

Thaís A, Frank L, Ignacio M, Miquel RC, Itxaso M, Charles N, John P, Monica VR, Miguel LH, and Alfons M. 2014. Herpes simplex virus encephalitis is a trigger of brain autoimmunity. *Annals of Neurology* 75:317-323.

Tiwari V, and Shukla D. 2010. Phosphoinositide 3 kinase signalling may affect multiple steps during herpes simplex virus type-1 entry. *Journal of General Virology* 91:3002-3009.

Trierweiler C, Hockenjos B, Zatloukal K, Blum HE, Wagner EF, and Hasselblatt P. 2013. 85 THE TRANSCRIPTION FACTOR c-JUN/AP-1 PROMOTES HBV-RELATED LIVER TUMORIGENESIS IN MICE. *Cell Death & Differentiation* 58:S38-S38.

Wald A, and Ashleymorrow R. 2002. Serological Testing for Herpes Simplex Virus (HSV)–1 and HSV-2 Infection. *Clinical Infectious Diseases* 35:S173.

Wang L, Dai W, and Lu L. 2011a. Hyperosmotic stress-induced corneal epithelial cell death through activation of Polo-like kinase 3 and c-Jun. *Investigative Ophthalmology & Visual Science* 52:3200-3206.

Wang L, Payton R, Dai W, and Lu L. 2011b. Hyperosmotic stress-induced ATF-2 activation through Polo-like kinase 3 in human corneal epithelial cells. *Journal of Biological Chemistry* 286:1951-1958.

Wang SH, Yeh SH, Shiau CW, Chen KF, Lin WH, Tsai TF, Teng YC, Chen DS, and Chen PJ. 2015. Sorafenib Action in Hepatitis B Virus X-Activated Oncogenic Androgen Pathway in Liver through SHP-1.

Journal of the National Cancer Institute 107.

Xu A, Li Y, Zhao W, Fei H, Li X, Lan S, Wei C, Yang A, Wu S, and Bei Z. 2017. PHP14 regulates hepatic stellate cells migration in liver fibrosis via mediating TGF-β1 signaling to PI3Kγ/AKT/Rac1 pathway. *Journal of Molecular Medicine* 96:119-133.

Yung-Chia C, Wen-Chi S, Jing-Ying H, Ti-Chun C, King-Song J, Keigo M, and Lai MMC. 2010. Polo-like kinase 1 is involved in hepatitis C virus replication by hyperphosphorylating NS5A. *Journal of Virology* 84:7983-7993.

Zakia K, Anna Z, Jeroen DH, Spaink HP, Schaaf MJM, and Meijer AH. 2013. Deficiency in hematopoietic phosphatase ptpn6/Shp1 hyperactivates the innate immune system and impairs control of bacterial infections in zebrafish embryos. *Journal of Immunology* 190:1631-1645.

Zapp D, Loos D, Feucht N, Khoramnia R, Tandogan T, Reznicek L, and Mayer C. 2018. Microbial keratitis-induced endophthalmitis: incidence, symptoms, therapy, visual prognosis and outcomes. *Bmc Ophthalmology* 18:112.

Zhen-Ling W, Xiao-Hua W, Li-Fang S, Yong-Sheng W, Xiao-Hong H, You-Fu L, Zhi-Zhi C, Jin K, Xiao-Dong P, and Chun-Mei H. 2009. Phosphoinositide 3-kinase gamma inhibitor ameliorates concanavalin A-induced hepatic injury in mice. *Biochemical & Biophysical Research Communications* 386:569-574.

Zhi Qiang Y, Audrey EV, Waggoner SN, Cale EM, and Hahn YS. 2004. Direct binding of hepatitis C virus core to gC1qR on CD4+ and CD8+ T cells leads to impaired activation of Lck and Akt. *Journal of Virology* 78:6409-6419.

Zhong L, Shu W, Dai W, Gao B, and Xiong S. 2017. Reactive Oxygen Species-Mediated c-Jun NH2-Terminal Kinase Activation Contributes to Hepatitis B Virus X Protein-Induced Autophagy via Regulation of the Beclin-1/Bcl-2 Interaction. *Journal of Virology* 91: e00001-00017.

Zou Y, Xiong JB, Ma K, Wang AZ, and Qian KJ. 2017. Rac2 deficiency attenuates CCl4-induced liver injury through suppressing inflammation and oxidative stress. *Biomedicine & pharmacotherapy = Biomedecine & pharmacotherapie* 94:140.

398

399

400 **Figure legends**

401 **Figure 1.** The box plots before (left) and after (right) normalization.

402 **Figure 2.** The histogram (A) and Venn diagram (B) of the differentially expressed genes (DEGs) identified for
403 the four time point groups (D1, D3, D5, and D7). In the histogram, red and green separately represent up-
404 regulated genes and down-regulated genes.

405 **Figure 3.** The significant clusters (cluster 1, 2, 3, 4, 5, 6, 7, and 8) obtained from time series expression
406 analysis. The squares represent different clusters. The number at the upper left of the square indicates the serial
407 number of each cluster. The black broken line in the square indicates the overall expression trend of the genes
408 in the cluster. The number in the lower left of the square indicates the significant p-value of gene expression
409 similarity in the cluster. The number in the lower right of the square indicates the number of genes involved in
410 the cluster.

411 **Figure 4.** The protein-protein interaction (PPI) network. The size of the network node indicates the degree of
412 the node. The larger the node, the higher the degree of the node is.

413 **Figure 5.** The eight significant modules identified from the protein-protein interaction (PPI) network. M1, M2,
414 M3, M4, M5, M6, M7, and M8 represent module 1, module 2, module 3, module 4, module 5, module 6,
415 module 7, and module 8, respectively.

Table 1(on next page)

Table 1. The results of enrichment analysis for the differentially expressed genes (DEGs) involved in the three clusters.

Table 1. The results of enrichment analysis for the differentially expressed genes (DEGs) involved in the three clusters.

Term	Count	P-value	FDR
GO:0006955~immune response	70	1.41E-09	3.96E-06
GO:0002478~antigen processing and presentation of exogenous peptide antigen	11	1.13E-06	1.06E-03
GO:0048002~antigen processing and presentation of peptide antigen	13	1.97E-06	1.39E-03
GO:0019884~antigen processing and presentation of exogenous antigen	12	1.11E-06	1.56E-03
GO:0001775~cell activation	36	3.15E-05	1.76E-02
GO:0019221~cytokine-mediated signaling pathway	14	8.30E-05	3.29E-02
GO:0045321~leukocyte activation	32	9.64E-05	3.34E-02
GO:0050778~positive regulation of immune response	23	1.42E-04	4.35E-02
mmu04650:Natural killer cell mediated cytotoxicity	26	2.14E-06	1.80E-04
mmu04612:Antigen processing and presentation	22	1.91E-06	3.21E-04
mmu04514:Cell adhesion molecules (CAMs)	27	5.16E-05	2.17E-03
mmu04660:T cell receptor signaling pathway	21	3.58E-04	8.56E-03
mmu04060:Cytokine-cytokine receptor interaction	34	4.61E-04	9.64E-03
mmu04630:Jak-STAT signaling pathway	24	7.18E-04	1.33E-02
mmu04662:B cell receptor signaling pathway	15	1.96E-03	3.25E-02

Note: GO, Gene Ontology; FDR, false discovery rate.

Figure 1

Figure 1. The box plots before (left) and after (right) normalization.

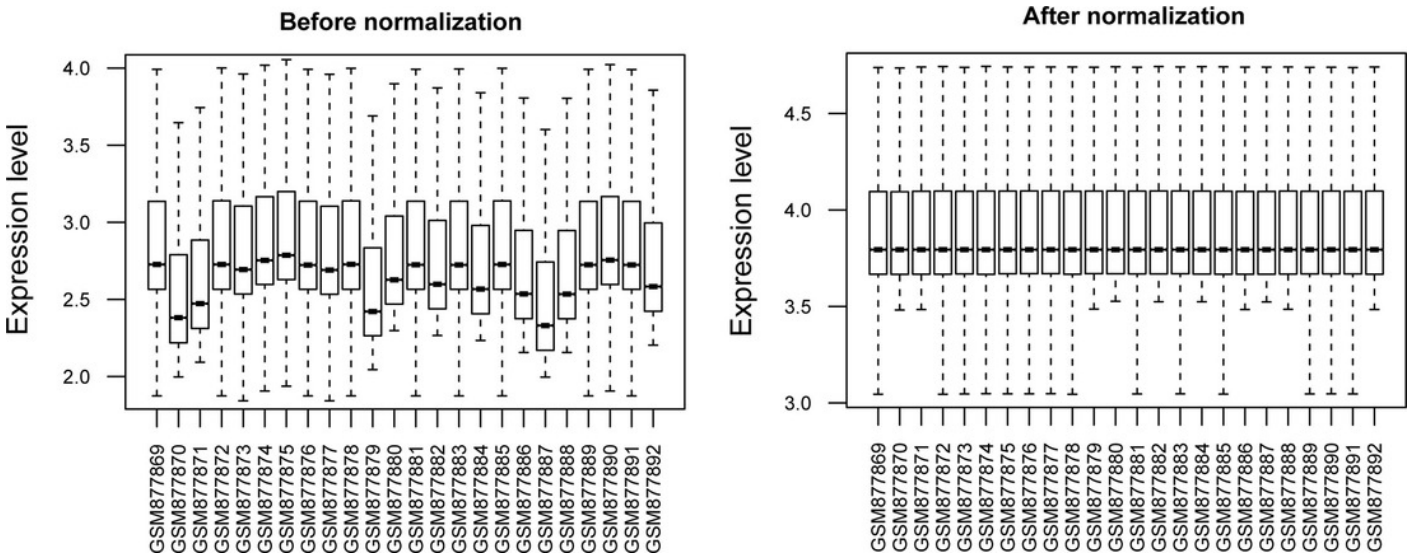

Figure 2

Figure 2. The histogram (A) and Venn diagram (B) of the differentially expressed genes (DEGs) identified for the four time point groups (D1, D3, D5, and D7).

In the histogram, red and green separately represent up-regulated genes and down-regulated genes.

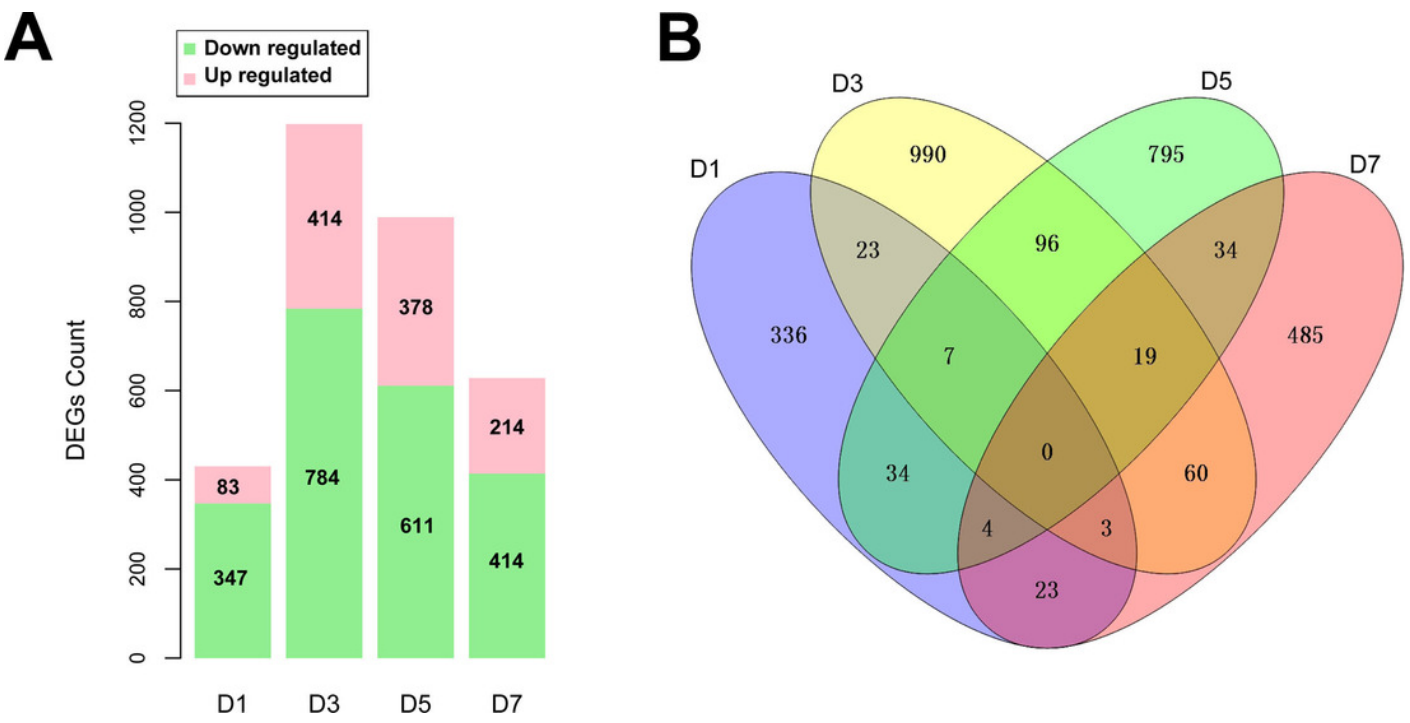

Figure 3

Figure 3. The significant clusters (cluster 1, 2, 3, 4, 5, 6, 7, and 8) obtained from time series expression analysis.

The squares represent different clusters. The number at the upper left of the square indicates the serial number of each cluster. The black broken line in the square indicates the overall expression trend of the genes in the cluster. The number in the lower left of the square indicates the significant p-value of gene expression similarity in the cluster. The number in the lower right of the square indicates the number of genes involved in the cluster.

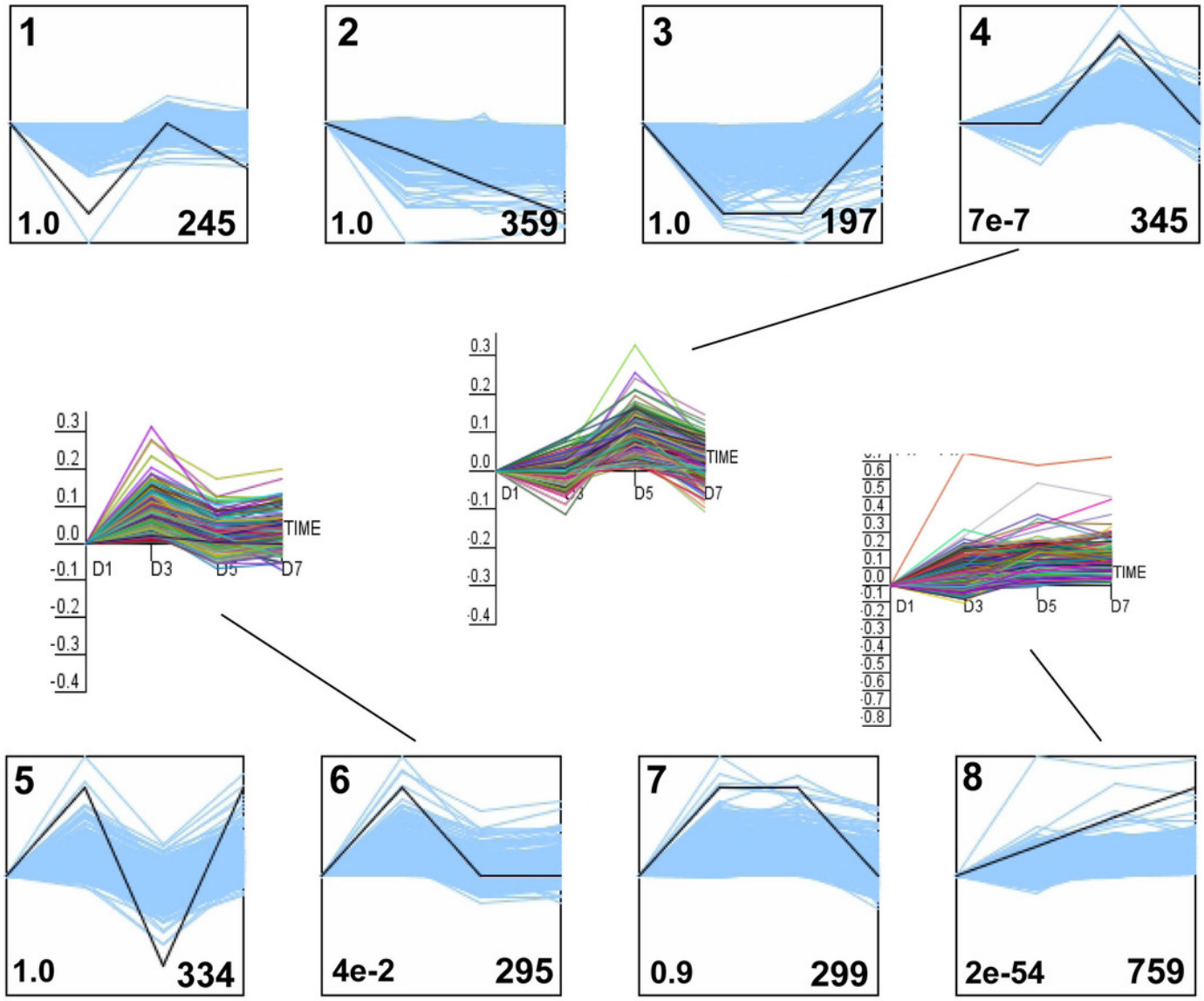

Table 2(on next page)

Table 2. The results of enrichment analysis for the nodes in the protein-protein interaction (PPI) network.

Table 2. The results of enrichment analysis for the nodes in the protein-protein interaction (PPI) network.

Term	Count	P-value	FDR
GO:0006955~immune response	51	1.55E-14	2.71E-11
GO:0006952~defense response	42	4.54E-10	7.93E-07
GO:0001775~cell activation	30	5.80E-10	1.01E-06
GO:0045321~leukocyte activation	28	8.55E-10	1.49E-06
GO:0002684~positive regulation of immune system process	24	1.01E-07	1.77E-04
GO:0006793~phosphorus metabolic process	57	1.05E-07	1.84E-04
GO:0006796~phosphate metabolic process	57	1.05E-07	1.84E-04
GO:0046649~lymphocyte activation	22	4.71E-07	8.23E-04
GO:0006468~protein amino acid phosphorylation	45	5.40E-07	9.44E-04
GO:0010941~regulation of cell death	41	8.01E-07	1.40E-03
GO:0016310~phosphorylation	48	8.77E-07	1.53E-03
GO:0043067~regulation of programmed cell death	40	1.82E-06	3.17E-03
GO:0042981~regulation of apoptosis	39	3.39E-06	5.92E-03
GO:0009611~response to wounding	29	3.58E-06	6.25E-03
GO:0006954~inflammatory response	22	6.69E-06	1.17E-02
mmu04650:Natural killer cell mediated cytotoxicity	26	2.09E-09	3.26E-07
mmu04612:Antigen processing and presentation	19	7.11E-07	5.55E-05
mmu04060:Cytokine-cytokine receptor interaction	33	9.03E-07	4.69E-05
mmu04514:Cell adhesion molecules (CAMs)	25	1.04E-06	3.25E-05
mmu04660:T cell receptor signaling pathway	21	2.25E-06	5.84E-05
mmu04662:B cell receptor signaling pathway	15	5.34E-05	9.26E-04
mmu04630:Jak-STAT signaling pathway	21	1.05E-04	1.63E-03
mmu04620:Toll-like receptor signaling pathway	16	1.61E-04	2.28E-03
mmu04670:Leukocyte transendothelial migration	17	4.02E-04	4.82E-03
mmu04664:Fc epsilon RI signaling pathway	13	9.95E-04	1.03E-02
mmu04062:Chemokine signaling pathway	21	1.15E-03	1.05E-02
mmu04621:NOD-like receptor signaling pathway	11	1.22E-03	1.05E-02
mmu04510:Focal adhesion	22	1.38E-03	1.13E-02

Note: GO, Gene Ontology; FDR, false discovery rate.

Figure 4

Figure 4. The protein-protein interaction (PPI) network.

The size of the network node indicates the degree of the node. The larger the node, the higher the degree of the node is.

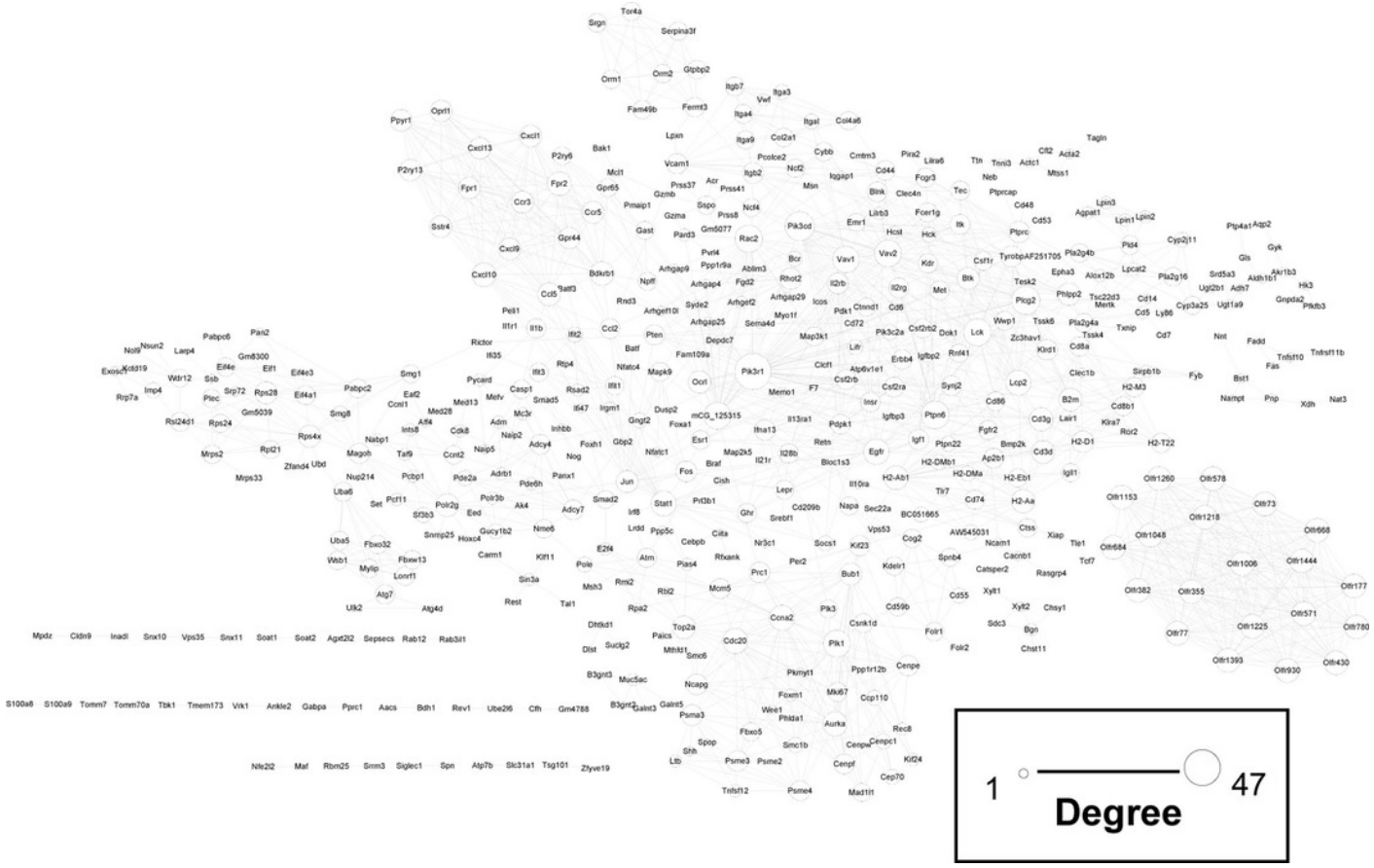

Table 3(on next page)

Table 3. The topology parameters of the top 10 nodes in the protein-protein interaction (PPI) network.

Table 3. The topology parameters of the top 10 nodes in the protein-protein interaction (PPI) network.

ID	Average Shortest Path Length	Betweenness Centrality	Closeness Centrality	Degree
Pik3r1	3.276	0.157	0.305	47
Pik3cd	3.534	0.049	0.283	31
Plcg2	3.557	0.146	0.281	29
Ptpn6	3.589	0.064	0.279	28
Lck	3.697	0.050	0.270	27
Rac2	3.744	0.060	0.267	27
mCG_125315	3.559	0.138	0.281	26
Plk1	4.414	0.041	0.227	26
Vav2	3.562	0.035	0.281	26
Vav1	3.581	0.039	0.279	25

Figure 5

Figure 5. The eight significant modules identified from the protein-protein interaction (PPI) network.

M1, M2, M3, M4, M5, M6, M7, and M8 represent module 1, module 2, module 3, module 4, module 5, module 6, module 7, and module 8, respectively.

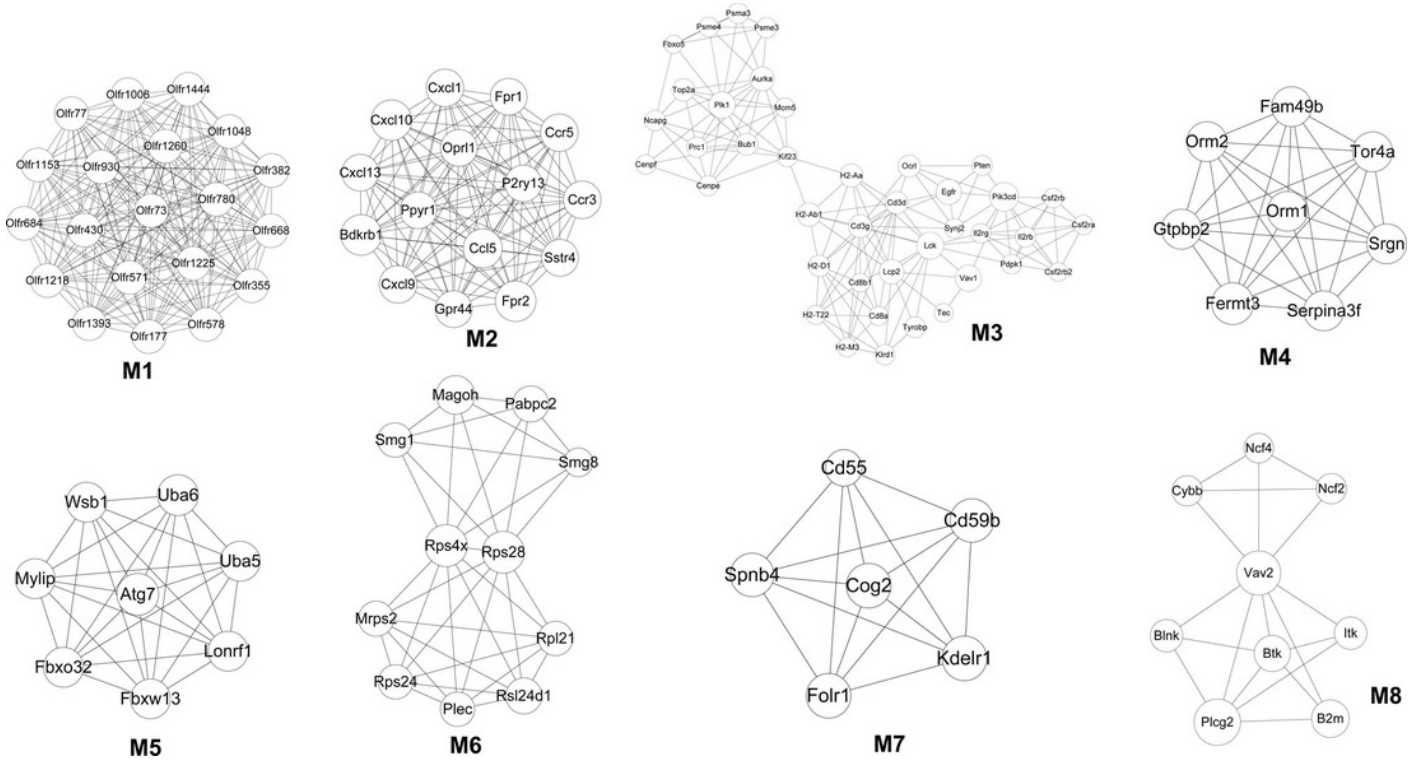

Table 4(on next page)

Table 4. The parameter information of the eight significant modules identified from the protein-protein interaction (PPI) network.

Table 4. The parameter information of the eight significant modules identified from the protein-protein interaction (PPI) network.

Module	Score	Node	Edges	Node IDs
1	9.5	20	190	Olfr578,Olfr1260,Olfr73,Olfr1444,Olfr1153,Olfr382,Olfr930,Olfr668,Olfr430,Olfr1393,Olfr571,Olfr1218,Olfr684,Olfr177,Olfr1048,Olfr780,Olfr355,Olfr77,Olfr1006,Olfr1225
2	7	15	105	Cxcl13,Ccr5,Ccr3,Sstr4,Bdkrb1,Ppyr1,Fpr1,P2ry13,Ccl5,Gpr44,Cxcl1,Cxcl9,Fpr2,Cxcl10,Oprl1
3	3.55	40	142	Cenpe,Plk1,Synj2,Mcm5,Psme4,Ncapg,Cd3g,H2-D1,Lcp2,Tyrobp,Vav1,Cenpf,Tec,Aurka,Il2rb,Csf2rb2,Cd8b1,H2-Ab1,Cd3d,Prc1,Bub1,Pten,Pdpk1,H2M3,Csf2ra,Kif23,Pik3cd,Klrd1,Psma3,Psme3,Fbxo5,Cd8a,H2-Aa,Top2a,Csf2rb,H2-T22,Il2rg,Lck,Ocrl,Egfr,
4	3.5	8	28	Fermt3,Srgn,Orm2,Tor4a,Serpina3f,Orm1,Fam49b,Gtpbp2
5	3.5	8	28	Uba5,Fbxw13,Wsb1,Uba6,Mylip,Lonrf1,Fbxo32,Atg7
6	3.182	11	35	Mrps2,Rsl24d1,Magoh,Plec,Smg8,Smg1,Rps24,Pabpc2,Rpl21,Rps28,Rps4x
7	2.5	6	15	Cd59b,Spnb4,Folr1,Kdelr1,Cd55,Cog2
8	2	9	18	Ncf2,Btk,Ncf4,Plcg2,B2m,Vav2,Cybb,Itk,Blnk